Environmental Science
Nano

ROYAL SOCIETY
OF CHEMISTRY | Celebrating
IYPT 2019

PAPER
J. A. J. Meesters *et al.*
A model sensitivity analysis to determine the most important
physicochemical properties driving environmental fate and exposure of
engineered nanoparticles

A model sensitivity analysis to determine the most important physicochemical properties driving environmental fate and exposure of engineered nanoparticles†

J. A. J. Meesters, [ID] *[ab] W. J. G. M. Peijnenburg, [ID] [bc] A. J. Hendriks,[a]
D. Van de Meent[a] and J. T. K. Quik [ID] [b]

New insights in the environmental exposure to nanomaterials have been gained from simulations with recently developed multimedia fate models: atmospheric concentrations are relatively low, and sedimentation in the water column is dominated by aggregation with natural particles, whereas soils and sediments are identified as environmental sinks. These model simulations however have only been performed for a limited set of nanomaterials. It is not yet clear to what extent the new insights gained from the limited set of evaluated nanomaterials generally apply to all nanomaterials. A sensitivity analysis was therefore performed of the nanomaterial environmental fate model SimpleBox4nano in order to investigate to what extent its model simulations are driven by the physicochemical properties of a nanomaterial. Sensitivity plots are drawn to quantify how the nanomaterial physicochemical properties specific weight, diameter, Hamaker constant, transformation rate constant, and attachment efficiency with natural particles, relate to (i) simulated key environmental fate processes such as deposition, filtration, and attachment and (ii) predicted free, bioavailable and total concentrations in air, water, sediment and soil. The critical transformation rate constant and attachment efficiency, at which these processes become dominant for prediction of the exposure concentrations are derived. Although exposure modelling is only part of a full environmental risk assessment of ENPs, they deliver insightful results for further development of ERA approaches by indicating to what extent ENP physicochemical properties affect predicted environmental exposure.

Environmental significance

A sensitivity analysis with the SimpleBox4nano model is performed to examine what physicochemical properties of nanoparticles are most important in simulating their environmental fate and exposure, which were found to be the rate at which nanoparticles transform and the efficiency with which engineered nanoparticles attach to natural particles. The explanations of complex relationships between the modelled environmental exposure concentrations and these physicochemical properties provide valuable insight in the required accuracy of measurement methods and reveal patterns of speciation relevant for effect assessment of nanoparticles.

Introduction

The nanotechnology industry is rapidly developing engineered nanoparticles (ENPs) that are applied in a great variety of consumer and industrial products.[1] Release of ENPs to the environment is anticipated in production, use and disposal.[2] However, the environmental fate, bioavailability, bioaccumulation, toxicity and thus the environmental risk of ENPs require more knowledge in order to be fully understood,[3] which raises concern about unforeseen environmental and (eco)toxicological consequences.[4,5] Any misconception on human and environmental risks may seriously hamper application of nanotechnology including promising technologies in energy innovation and sustainable development.[4,6] Hence, the research agenda in safety assessment of nanomaterials is top priority in governments, the private sector and industry[7–9] in order to fully exploit the benefits of nanotechnology without compromising human and environmental health.[4,5,8–11]

[a] *Institute for Water and Wetland Research, Department of Environmental Science, Radboud University Nijmegen, P.O. Box 9010, NL-6500 GL, Nijmegen, The Netherlands. E-mail: joris.meesters@rivm.nl*
[b] *National Institute of Public Health and the Environment RIVM, P.O. Box 1, 3720 BA, Bilthoven, The Netherlands*
[c] *Institute of Environmental Sciences (CML), Leiden University, PO Box 9518, 2300 RA, Leiden, The Netherlands*
† Electronic supplementary information (ESI) available. See DOI: 10.1039/c9en00117d

This journal is © The Royal Society of Chemistry 2019

Environ. Sci.: Nano, 2019, **6**, 2049–2060 | 2049

Environmental exposure estimation of ENPs is an important component in this research agenda.[8,12] Novel multimedia fate models have been developed to gain more insight in the environmental fate of nanomaterials and to predict exposure concentrations.[13–23] A new generation of models, such as MendNano,[13,14] NanoDUFLOW,[24] RedNano,[25] nanoFate,[26] WASP8[27–30] and SimpleBox4nano (SB4N),[15,31,32] are appropriate for environmental exposure estimation[32] and have revealed some important new insights in environmental fate and exposure of ENPs:[33–40] (i) atmospheric concentrations are low due to effective removal and negligible inflow from water or soil,[2,13–15,32] (ii) hetero-aggregation with natural particles is the dominant mechanism for settling from the water column to sediment,[41–44] (iii) soils and sediments are environmental sinks,[13–15] (iv) only a small fraction of ENPs emitted to the environment will persist in a free pristine state,[15–17,45] and (v) high 'hotspot' concentrations are predicted in close proximities to the locations of environmental release.[45]

However, the novel ENP fate models have only been applied for predicting the fate and concentrations of often the same specific nanomaterials, such as C_{60}, graphene, carbon nanotubes (CNTs) nano-Ag, -CeO$_2$, -TiO$_2$, -ZnO, that are selected for evaluation because of their relatively high availability of data compared to other nanomaterials.[12–17,19,24,27,28,30,32,44–46] Nanomaterials for which most data are available for performing risk assessment exercises are also the nanomaterials produced in the highest volumes.[22] Consequently, the priority in environmental risk assessment of nanomaterials is implicitly assigned to the most produced nanomaterials. Higher production volumes indeed lead to higher exposure estimates,[32] but similar considerations apply to nanomaterials with physicochemical properties inducing higher bioavailability, long range transport potential, or persistency.[47–50] Hence, the environmental exposure levels are not just related to the highest production volumes. The goal of this study is therefore to investigate the relationship between physicochemical properties, fate and exposure, in order to deliver new arguments in priority setting in environmental risk assessment and management of nanomaterials.[33,51,52]

Such an investigation is performed here by means of a sensitivity analysis of the multimedia fate model SimpleBox4nano (SB4N). SB4N is developed to simulate environmental exposure to nanomaterials at a screening level.[15] The SB4N model is beneficial for this exercise because it integrates the key environmental fate processes (deposition, attachment, filtration and transformation) of nanomaterials[53–55] into one matrix. The model algorithms of these key processes require five different physicochemical properties or functional assays as input: (i) specific weight, (ii) size, (iii) Hamaker Constant (iv) transformation rate constant, and (v) attachment efficiencies with natural particles.[32,56] In this study transformation is considered an overarching process defined by the transformation to another chemical or particle form which is no longer considered within the scope of the exposure assessment. This could for instance be dissolution, sulfidation or oxidation. Attachment to other particles is considered a speciation process that leads to another ENP species still considered within scope of the exposure assessment. Instead of performing separate exposure estimations for different nanomaterials, we argue that it is more effective to analyse the model sensitivity towards these five physicochemical properties. Such a sensitivity analysis is performed here by expressing simulated environmental concentrations of nanomaterials in the atmosphere, water, sediment and soil as a direct function of their physicochemical properties. The goal of these sensitivity analyses is to deliver appropriate simulation data to discuss general patterns and the importance of accurately characterizing the physicochemical properties of nanomaterials that predominantly affect the key fate processes of ENPs for the purpose of environmental exposure estimation and risk assessment.

Methods

Monte Carlo simulations

A sensitivity analysis has been performed by means of a Monte Carlo (MC) simulation with the software package of Oracle Crystal Ball[57] on the SB4N model.[32] These simulations are performed using the SB4N concept model from Meesters et al.[56] with probabilistic model parameter settings to describe landscape characteristics of the environmental system.[31,32] The model solves mass balance equations for a steady-state situation in all compartments and species through matrix algebra:[15,32,58]

$$m = -A^{-1}e \tag{1}$$

Here e (kg s^{-1}) is the vector of emission rates of engineered nanoparticles (ENPs) into the environment. The system matrix A (s^{-1}) represents first-order rate constants for (i) transport between compartments and to media outside the system, (ii) formation of relevant ENP species due to attachment of ENPs to natural particles, and (iii) transformation to a different chemical or particle form.[15] Although in the original model concept[15] transformation was only considered in terms of dissolution or underlying chemical reactions, this is not always the case. For instance other transformation processes, such as biodegradation[47] or photodegradation, are also described by this transformation rate constant.[59] The rate constants for the other processes included in the system matrix are calculated with specific model algorithms ((ESI†) section C).[15] These include the environmental fate and speciation of ENPs as emitted in a free and pristine state, as hetero-aggregates with natural colloid particles (<450 nm[60]), and as ENPs attached to the surface of natural coarse particles (>450 nm[60]).[15] Natural variability of the environmental system is represented in the MC simulations by probability distributions assigned to the model parameters that define the environmental system (ESI† chapter E).[32]

Model input parameters that refer to the physicochemical properties have been inserted as ranges covering any ENP

that can be described by a sphere (Table 1). This is based on the assumption that an equivalent sphere, *e.g.* using the hydrodynamic diameter adequately describes non-spherical particles, such as CNTs.[30]

The predicted environmental concentrations (PECs) of the different ENP species are evaluated in three separate emission scenarios of 1 t per year emission of pristine (free) ENPs to (i) water, (ii) soil and (iii) air. Each emission scenario is simulated in a model run of 10 000 iterations. The MC simulation delivers output by means of an extract data sheet representing each iteration in the MC run. The data consist of 10 000 data points for (i) the range of randomly selected values for the physicochemical properties of ENPs given in Table 1, (ii) the randomly selected values from the probability distributions representing the natural variability of the environmental system,[32] (iii) the calculated rate constants for the key environmental processes included in matrix *A*, (iv) the calculated mass balance of ENPs per compartment and their speciation (pristine ENP, colloidal or coarse heteroagglomerate). PECs are calculated by dividing the steady state mass with the volume (m^3) or dry weight (kg) of the environmental medium. Here, the PECs in air are plotted for the emission scenario to air only and the PECs in soil are plotted for the emission scenario to soil only. The PECs in water and sediment are displayed for the emission scenario to water only. The influence of physicochemical properties on environmental fate and exposure is visualized by plotting the extracted data.

The bioavailable concentrations are interpreted as the sum of the concentrations of free ENPs and the ENPs heteroaggregated with natural colloids (<0.45 μm),[32] because in environmental risk regulations the bioavailable fraction of a chemical or metal compound is arbitrary defined as the fraction that "is able to pass through a filter of <0.45 μm".[66] It is still uncertain whether the arbitrary split of <0.45 μm applies to nanomaterials.[67] ENPs that are attached to coarse particles are included in the total predicted exposure concentrations per environmental compartment, since it is uncertain whether the coarse attached ENPs can be treated as non-bioavailable and essentially harmless or not.[32,67]

Explaining model sensitivity

Scatter plots are drawn from the extract data of the MC simulations to express the sensitivity between the physicochemical

Table 1 Physicochemical property ranges for a hypothetical ENP that covers all types of ENPs

Physicochemical property	Range	Unit	Ref.
Diameter	1–100	nm	61, 62
Transformation rate constant	10^{-20}–10^{-3}	10^log (s^{-1})	47
Attachment efficiency	10^{-10}–1	10^log (−)	63, 64
Density	900–10 000	kg m^{-3}	*a*
Hamaker constant	10^{-21}–10^{-19}	10^log (J)	65

a A derived as order of magnitude for solid materials.

properties of ENPs and their PECs simulated with SB4N. In cases such sensitivity plots only display noise and intercept, it is interpreted that the PEC is not sensitive to the physicochemical property. Linear and more complex relationships displayed in the sensitivity plots are further analysed by considering the original mass balance equations simulated in SB4N. The mass balance (g) of free, bioavailable and total ENPs are simulated in SB4N with emission volumes (g s^{-1}) and the calculated rate constants (s^{-1}) for the environmental fate process responsible for the transport, speciation and removal of ENPs. Since, emission volumes are fixed in the MC simulations, any sensitivity between PECs and physicochemical properties displayed is due to the derived rate constants. Therefore, in order to explain the sensitivity plots that show linear or more complex relations, it is first determined what environmental fate processes are dominant. This is done by determining their respective rate constants available in the MC extract data, *i.e.* the environmental fate process with the highest rate constants represents the dominant processes (ESI† chapter B). Next, it is addressed how the physicochemical properties of ENP are included in SB4N's algorithm to derive the rate constants for these dominant fate processes. As such, the sensitivity of PECs to physicochemical properties is explained with simplified equations that only consider the dominant fate process. These simplified equations are then verified by comparing their outcomes against the PECs simulated with SB4N's original matrix algebra (ESI† section C1).

Results and discussion

Sensitivity of predicted environmental concentrations

The results of the sensitivity analyses are quantitatively expressed in sensitivity plots that display the predicted free, bioavailable and total concentrations in air, water, sediment and soil as a function of the ENP's physicochemical properties diameter, density, transformation rate constant, attachment efficiency with natural particles, and Hamaker constant with natural particles in water and porous media (ESI† chapter A). The sensitivity of the PECs are summarized as (i) insensitive (scatter plots only display an intercept and noise), (ii) linear, and (iii) complex functions (Table 2).

Air

The PEC in air of free ENPs is found sensitive to the ENP diameter (Table 2, ESI† Fig. A1). The function plotted between diameter and the PEC of free ENPs is rather complex as an increasing ENP diameter yields an increase of the PEC itself as well as the range of the simulated outcomes (ESI† section A).

Free concentration in air. From the extracted data of the MC simulations it is retrieved that coagulation with fine aerosol particles and outflow of air are the dominant fate processes removing free ENPs from air (ESI† section B1). The outflow of air is included in SB4N as an advective transport process that does not depend on any physicochemical property of the ENP, whereas the simulated rate constant for coagulation with fine aerosols is the sum of the rate constants for

Table 2 The relation between nanomaterial physicochemical properties and predicted free, bioavailable and total concentrations in air, water and soil derived from sensitivity plots that show no relation (N), linear relation (L) or a complex relation (C) or whether the property is not included in SB4N to derive the PEC (–)

Predicted environmental concentration	Physicochemical property of nanomaterial				
	Diameter (nm)	Density (kg m^{-3})	Transformation rate constant (s^{-1})	Attachment efficiency (–)	Hamaker constant (J)
Air (g m^{-3})					
Free	C	N	N	—	—
Bioavailable	N	N	N	—	—
Total	N	N	N	—	—
Water (g m^{-3})					
Free	N	N	C	C	—
Bioavailable	N	N	C	N	—
Total	N	N	C	N	—
Sediment (g kg^{-1})					
Free	L	C	C	C	N
Bioavailable	L	C	C	N	N
Total	L	N	C	C	N
Soil (g kg^{-1})					
Free	L	N	C	C	N
Bioavailable	L	N	C	C	N
Total	L	N	C	C	N

coagulation with nucleation (~20 nm) and accumulation (~116 nm) mode aerosols.[15,68]

The rate constant for coagulation with accumulation mode aerosols decreases with ENP diameter, whereas coagulation with nucleation mode increases with ENP diameter (ESI† section B1). Moreover, coagulation with accumulation mode aerosols is dominant over coagulation with nucleation mode aerosols for smaller ENPs, whereas the opposite is the case for larger ENPs (ESI† section B1). The critical ENP diameter at which nucleation becomes dominant over accumulation is calculated to be 38 nm by median (95% CI = 21–60 nm). However, this only partially explains the sensitivity of free PECs in air towards ENP diameter. The rate at which smaller free ENPs coagulate with accumulation mode aerosols is also higher than the sum of all other fate processes removing free ENPs from the air, but the critical ENP diameter at which this is no longer the case is calculated to be 34 nm by median (95% CI = 7–55 nm). As such, the sensitivity of PECs for free ENPs in air can be explained: small ENPs rapidly coagulate with accumulation mode aerosols, but the respective rate constant decreases with ENP diameter. The PECs of free ENPs larger than a critical diameter of 34 nm are most strongly determined by outflow of air and coagulation with nucleation mode aerosols, which is an atmospheric fate process simulated to be more strongly subjected to variability than coagulation with accumulation mode aerosols (ESI† section B1). The PECs of free ENPs are inversely proportional to the rate constants of the fate processes removing them. Therefore, PECs of free ENPs in air increase with ENP diameter <34 nm, but for larger ENPs the ranges in the simulated outcomes increase as well (ESI† Fig. 1; ESI section B1).

Bioavailable and total concentration in air. The fast coagulation with fine aerosol particles also explains why SB4N simulates the bioavailable concentration to be equal to the total concentration (ESI† section B1). The model calculates only a

small fraction of ENPs to coagulate with the non-bioavailable coarse mode aerosols as simulated rate constants for coagulation with fine aerosols are at least a factor 1000 larger.[32] As such, the non-bioavailable fraction of the total concentration of ENPs is marginal (by median 1.0×10^{-4} and 95 CI = 1.8×10^{-7}–2.5×10^{-3}).

Water

The free, bioavailable and total concentrations predicted for the water compartment are sensitive to the transformation rate constant of the ENP. Furthermore, the free concentrations are also sensitive to the ENP's attachment efficiency with natural particles. The sensitivities plotted between the PECs in water and the transformation rate constant and/or attachment efficiency are complex functions (Table 2; ESI† section A).

Free concentration in water. The most important aquatic fate processes that determine the PEC of free ENPs in water in SB4N are outflow of water, sedimentation, transformation and attachment to natural colloidal and coarse particles (ESI† section B2). Water outflow is simulated as the dominant aquatic fate process that determines the PEC of free ENPs in water for ENPs with low transformation and attachment rate constants (ESI† Fig. S7). However, there appear to be critical transformation rate constants and critical attachment efficiencies at which transformation, colloid aggregation and coarse attachment become dominant over water outflow (ESI† Fig. 8). Attachment efficiency is a physicochemical property of ENPs that is included as a constant in SB4N's algorithm to simulate hetero-aggregation with natural colloids and attachment to coarse particles, whereas the transformation rate constant of ENPs is directly inserted as an input parameter. The critical attachment efficiency at which attachment to natural colloid and coarse particles is the dominant

2052 | *Environ. Sci.: Nano*, 2019, **6**, 2049–2060

This journal is © The Royal Society of Chemistry 2019

aquatic fate process is calculated to be 1.1×10^{-4} by median (95% CI = 7.5×10^{-5}–1.6×10^{-4}) for ENPs that do not dissolve. The critical transformation rate constant at which transformation is the dominant aquatic fate process is calculated to be 3.5×10^{-7} by median (95% CI = 1.7×10^{-7}–7.4×10^{-7}) for stable ENPs that do no attach to natural particles ($\alpha = 0$). However, such critical attachment efficiencies and transformation rate constants become complementary for ENPs that are soluble, instable ($\alpha > 0$) or both (ESI† section C4) which are analytically derived as:

$$k_{\text{trans(crit.free in water)}} = \alpha\left(f_{\text{ENP-colloids}} + f_{\text{ENP-Coarse}}\right) + k_{\text{set.free}} + k_{\text{out.water}} \quad (2)$$

and

$$\alpha_{\text{crit.free in water}} = \frac{k_{\text{trans}} + k_{\text{set.free}} + k_{\text{out.water}}}{f_{\text{ENP-colloids}} + f_{\text{ENP-Coarse}}} \quad (3)$$

Here, α is the attachment efficiency between ENP and natural particles, k_{trans} the transformation rate constant of the ENP, $k_{\text{set.free}}$ the rate constant for settling of free ENPs, $k_{\text{out.water}}$ the rate constant for water outflow, $f_{\text{ENP-colloids}}$ the collision frequency between ENPs and natural colloids, and $f_{\text{ENP-coarse}}$ the collision frequency between ENPs and natural coarse particles.

The complementary impact of transformation and attachment of ENPs to natural particles explains the complex functions displayed in the sensitivity plots for the PECs of free ENPs in water to transformation rate constant and attachment efficiency (ESI† Fig. 2). The PEC of free ENPs in water is proportional to the inverse of the sum of the rate constants for the aquatic fate processes removing free ENPs from the water column. Attachment to natural particles linearly increases with increasing attachment efficiency (ESI† Fig. 8). Consequently, the PEC of free ENPs in water linearly decreases with increasing attachment efficiencies greater than the critical attachment efficiency (Table 2; ESI† Fig. 2). The same principle applies to the sensitivity between the PEC of free ENPs in water to transformation rate constant (Table 2; ESI† Fig. 2).

Total concentration in water. The total PEC of ENPs in the water column is inversely proportional to the sum of the rate constants derived for the aquatic fate processes removing ENPs from water, which are transformation, the settling of free colloid-aggregated and coarse-attached ENPs, and the outflow of water (Table 2, ESI† section C4). The total PEC of ENPs in water appears to be sensitive to transformation rate constant only, for which the respective sensitivity plot displays a complex function (Table 2; ESI† section A). Transformation is the dominant process removing ENPs from water if the respective rate constant is greater than the sum of the rate constants the other process, which are the outflow of water to a continental scale ($k_{\text{out.water}}$) and the gravitational settling of free ENPs and ENPs attached to natural particles to sediment ($\sum k_{\text{set.total}}$), so that

$$k_{\text{trans(crit.total in water)}} = k_{\text{out.water}} + \sum k_{\text{set.total}} \quad (4)$$

The critical rate at which transformation is dominant ($k_{\text{trans(crit.total in water)}}$) is then calculated to be 3.8×10^{-7} by median (95% CI = 1.7×10^{-7}–1.7×10^{-6}, see ESI† section C4).[69] As such, the complex sensitivity of total concentrations in water to transformation rate constant can be explained. The predicted total concentration in water is linearly proportional to the inverse of the rate constants that are dominant in removing ENPs from the water column. The predicted total concentration thus decreases with increasing transformation rate constants that are greater than the derived critical transformation rate constant (ESI† section A).

Bioavailable concentration in water. The fraction of the predicted total concentration of ENPs in water that is bioavailable approaches 100%, whereas the non-bioavailable fraction is marginal (95% CI = 1.7×10^{-9}–0.029, see ESI† section C4). The predicted bioavailable concentrations are therefore (almost) equal to the predicted total concentrations (ESI† section C4). This can be explained with the underlying algorithms of SB4N that simulate the collisions between ENPs with natural colloids to occur more frequent than collisions with coarse particles. Instable ENPs are thus more prone to form a bioavailable hetero-aggregate <0.45 μm (Fig. 1A), whereas stable ENPs ($\alpha < 1.1 \times 10^{-4}$, i.e. critical attachment efficiency free ENPs) are prone to remain bioavailable in their free form. Consequently, the fraction of ENPs that attach to non-bioavailable coarse particles is marginal at any attachment efficiency (Fig. 1A). Hence, the bioavailable concentrations are (almost) equal to the total concentration, so that the critical transformation rate constant derived for the total concentration of ENPs in water (Fig. 3) is also suitable for the bioavailable concentration.

Sediment

The predicted concentrations of free ENPS in sediment are found to be sensitive to ENP size, density, transformation rate constant and attachment efficiency with natural particles. The bioavailable concentrations are found to be sensitive only to ENP size and transformation rate constant, whereas the total concentrations are sensitive to ENP size, attachment efficiency, and transformation rate constant (Table 2; ESI† section A).

Sediment is an environmental compartment for which no emission is expected.[15,32,58,70,71] Instead, ENPs emitted to the water column settle down in order to reach the sediments.[32,41,42,59,72] Hence, the fate of ENPs within the entire aquatic system needs to be considered in order to evaluate the influence of the physicochemical properties on ENP concentrations in the sediment compartment.[32] Exposure concentrations of ENPs in sediment are therefore more complex to predict compared to the other environmental compartments.[15,32,41,42,59,72]

Free concentration in sediment. The settling of ENPs in the water column is the only fate process considered from which free ENPs enter the sediment compartment (Table 2). The concentration of free ENPs in sediment is proportional
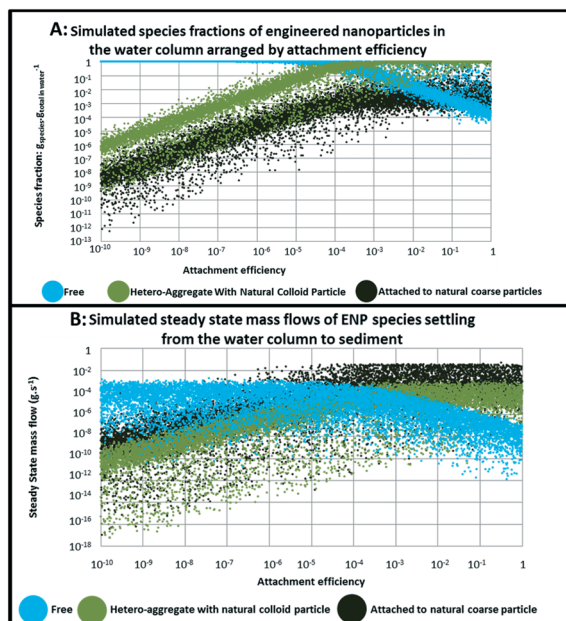
This journal is © The Royal Society of Chemistry 2019

Environ. Sci.: Nano, 2019, **6**, 2049–2060 | **2053**

Fig. 1 A: Extract sensitivity plot of attachment efficiency *vs.* the fractions of the concentrations in water that are free, hetero-aggregated with natural colloid particles, or attached to natural suspended coarse particles B: simulated steady state mass flows (g s⁻¹) of free, hetero-aggregated colloid, and coarse-attached ENPs as a function of attachment efficiency.

to the settling rate of free ENPs which is included in SB4N as a function of the Stokes settling velocity. The sensitivity of the predicted free concentrations towards ENP size and density is therefore explained by Stokes law that describes free ENPs that are larger and denser to settle faster:[73]

$$v_{\text{Strokes}} = \frac{2(\rho_{\text{ENP}} - \rho_{\text{water}})r_{\text{ENP}}^2 g}{9\mu_{\text{water}}} \quad (5)$$

ENPs with a specific weight smaller than the density of water (<1000 kg m⁻³) are calculated not to settle at all, but to remain floating.[73] Therefore, the concentrations of free ENPS in sediment are predicted to be zero if their density is less

than 1000 kg m⁻³. The proportionality of free concentrations to the Stokes settling rate also explains the increase with increasing ENP size, as larger ENPs are simulated to settle faster to the sediment compartment than small ENPs. Since the predicted bioavailable and total concentration of ENPs in sediment both comprise a fraction of free ENPs, these concentrations are also sensitive to ENP size but to a lesser extent (ESI† section C5).

The sensitivity of the free concentrations towards the transformation rate constant and attachment efficiency is explained by (i) the simulated frequencies for ENPs colliding with natural colloids and coarse particles in the water column, (ii) the frequencies of ENPs colliding with colloid particles and coarse particles in the sediment and (iii) the rate constants simulated for the other fate processes responsible for the removal of ENPs in both the water and the sediment compartment. Both attachment to natural particles and transformation remove free ENPs in the water column prior to settling as well as in the sediment compartment after settling (Table 2). The sensitivity of free ENP concentration towards attachment efficiency and transformation rate constant are therefore complementary to each other (ESI† section C5; Fig. 3A). Nonetheless, a critical attachment efficiency at which the predicted free concentration of not-transformable ENPs ($k_{\text{trans}} = 0$ s⁻¹) in sediment becomes sensitive to attachment efficiency is calculated to be 6.0×10^{-7} by median (95% CI = 3.2×10^{-8}–4.5×10^{-6}). A respective critical transformation rate constant for stable ENPs ($\alpha = 0$) is calculated to be 1.1×10^{-8} s⁻¹ by median (95% CI = 1.0×10^{-9}–5.5×10^{-8} s⁻¹, see ESI† section C5). The predicted free concentrations in sediment decrease with increasing transformation rate constant and attachment efficiency greater than the derived critical values (Fig. 3A), because both transformation and attachment are fate processes that remove ENPs as free species.

Bioavailable concentration in sediment. The predicted bioavailable concentrations in sediment are sensitive to ENP size and transformation, but not to attachment efficiency (Table 2 and Fig. 3B). The predicted free concentration is within the definitions of SB4N equal to the bioavailable concentration for ENPs that are stable ($\alpha = 0$), because the ENPs will not hetero-aggregate with natural colloids. As such, the critical rate at
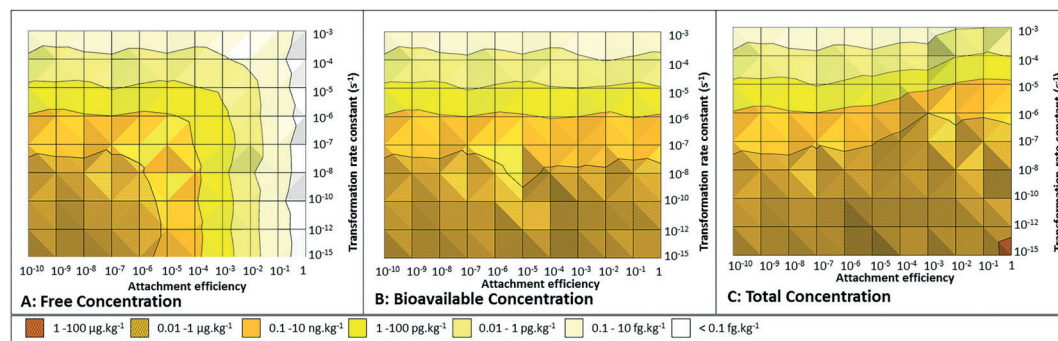

Fig. 2 Simulated (A) free, (B) bioavailable, and (C) total concentrations of ENPs in sediments arranged by attachment efficiency and transformation rate constant at 1 t per year emission to water.
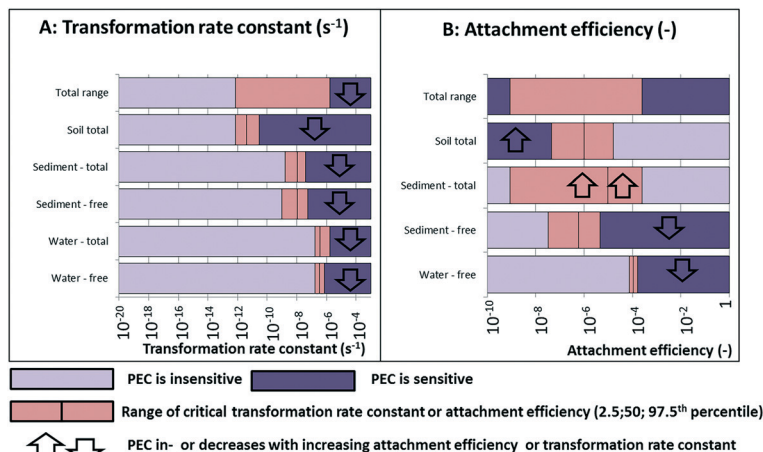
2054 | *Environ. Sci.: Nano*, 2019, **6**, 2049–2060

This journal is © The Royal Society of Chemistry 2019

Fig. 3 The complex relationships between predicted environmental concentrations (PECs) and (A) transformation rate constants and (B) attachment efficiencies explained with critical ranges at which PECs become sensitive.

which the predicted sediment concentration of free and stable ENPs become sensitive to transformation (1.1×10^{-8} s^{-1}) also applies to the bioavailable concentration (Fig. 3B, ESI† section C5). Moreover, the bioavailable concentration is insensitive to attachment efficiency, so that this critical transformation rate constant also applies to instable ENPs (Fig. 3B).

Total concentrations in sediment. The predicted total concentrations of ENPs in sediment are sensitive to transformation rate constant, attachment efficiency and size (Table 2). The speciation of ENPs in sediment is largely determined in the water column prior to settling (ESI† section C5). As such, the sensitivity to attachment efficiency can be explained by the speciation in the mass flow of ENPs settling from the water column to the sediment compartment (Fig. 2B). Free ENPs settle slower than ENPs hetero-aggregated with natural colloids or with natural coarse particles. The critical attachment efficiency at which the mass flow of settling free ENPs is less then ENP attached to natural particles is calculated to be 9.4×10^{-6} by median (95% CI = 8.8×10^{-10}–2.5×10^{-4}). Furthermore, the mass flow of settling ENPs attached to natural particles does not increase further for attachment efficiencies that are greater than the critical attachment efficiency at which hetero-aggregated ENPs are the dominant species in the water column that is calculated to be 1.1×10^{-4} (95% CI = 7.5×10^{-5}–1.6×10^{-4}, see Fig. 1A). The total concentration predicted for the sediment compartment is proportional to the total mass flow of settling ENPs (Fig. 1B), for which two critical attachment efficiencies are derived.

The predicted total concentration is therefore insensitive to attachment efficiencies <9.4×10^{-6} and >1.1×10^{-4}, but within this range the predicted concentrations increase with increasing attachment efficiency (Table 2, Fig. 1B and 2, ESI† section A).

Moreover, with $\alpha < 9.4 \times 10^{-6}$, the total mass flow of ENP settling to sediment mainly consists of free ENPs that settle slowly to the sediment compartment (Fig. 2B). The settling rate of free ENPs is a function of the ENP radius, which explains the sensitivity of the total concentration to ENP size (ESI† section A).

The sensitivity plot of the total sediment concentrations in relation to transformation rate constant displays a complex function, *i.e.* the total concentration is insensitive to low transformation rate constants, but decreases with increasing high transformation rate constants (Table 2, ESI† section A). This can be explained by comparing the transformation rate constant with the rate constants simulated for the other fate processes removing ENPs in the water column and sediment, such as burial and water outflow (Table 2). Transformation reduces the predicted concentration in sediment more than the combined reduction of the other fate processes if it proceeds faster than a critical rate (ESI† section C5). Such a critical transformation rate constant is derived to be by median 1.1×10^{-8} s^{-1} (95% CI = 1.6×10^{-9}–4.1×10^{-8} s^{-1}). The total concentration of ENPs is insensitive to transformation rate constants lower than this critical rate, but decreases with increasing transformation rate constants higher than this critical rate (ESI† section A, Fig. 2C).

Soil

The predicted free and total concentrations in soil are sensitive to the ENP's size, attachment efficiency with natural particles and transformation rate constant, whereas the bioavailable concentrations are found to be only sensitive to attachment efficiency and transformation rate constant (Table 2: ESI† section A). The total concentration is explained by the fraction of ENPs that attach to soil grains and their removal by transformation and erosion. Once attached to a soil grain, erosion is the only fate process that transports the ENPs out of the soil.[15] Such removal by erosion takes place within timescales of more than centuries, so that even at extreme low rates, transformation is the dominant removal mechanism for ENPs attached to soil grains.[32] A critical attachment efficiency at which the fraction of ENPs that is attached to soil grains is dominant, is derived to be 1.0×10^{-6} by median (95% CI = 4.4×10^{-8}–1.6×10^{-5}, see ESI† section C6). Consequently, the predicted total concentrations no

longer increase with attachment efficiencies higher than this critical attachment efficiency (ESI† section A). The critical transformation rate constant at which the concentration of ENPs attached to soil grains becomes sensitive to transformation is derived to be 4.1×10^{-12} s^{-1} (95% CI = 7.2×10^{-13}–3.0×10^{-11} s^{-1}). ENPs that are poorly transformable ($k_{trans} < 4.1 \times 10^{-12}$ s^{-1}) and effectively filtered by soil grains ($\alpha > 1.0 \times 10^{-6}$) are simulated to accumulate in soil so that the total concentrations of ENPs increase over time. Free ENPs and ENPs hetero-aggregated with natural colloids are simulated in SB4N to be less accumulative in soil as they are also subject to the more effective transport processes which remove ENPs from soil *via* run-off to surface waters and leaching to the deeper ground water layers.[15] Moreover, filtration is simulated to be dominant over hetero-aggregation with the natural colloids in soil pore water (ESI† section B3). Instable ENPs are as such more prone to accumulate by attaching to non-bioavailable soil grains than to attach to the bioavailable natural colloids in pore water. As such, the predicted concentrations of free and bioavailable ENPs in soil decrease with increasing attachment efficiency (Table 2; ESI† chapter A). However, the filtration frequency decreases weakly with ENP diameter (ESI† section C6), which explains why larger ENPs are simulated to be more bioavailable in soil.

Transformation rate constant and attachment efficiency most important

The predicted concentrations in water, sediment, and soil are found to be most sensitive to the transformation rate constant and attachment efficiency (Table 2). Moreover, the sensitivities to the transformation rate constant and attachment efficiency are complementary in the prediction of free ENPs in water, sediment and soil, as well as the predicted total concentration of ENPs in soil and sediment.

However, both the transformation rate constant and attachment efficiency are actually functional assays of the ENP that are difficult to characterize.[47,53] For instance metal ENPs transformation rate constants for dissolution depend on the surface chemistry of the ENP as affected by the environmental medium,[47,59] whereas attachment efficiencies depend on the environmental medium and the size, shape and surface of both the ENP and the natural particle it collides with.[63] The complexity of ENP transformation and attachment behaviour in environmental media is often dealt with by treating these processes as being uncertain and considering the worst-case outcome in predicted exposure.[28–30,32,44,47]

Nonetheless, it seems that this is an acceptable approach, because variations in predicted environmental exposure as a consequence of uncertain transformation rate constants or attachment efficiencies can be foreseen with sensitivity analyses that indicate what would be the most conservative PEC. Moreover, such uncertainty does not influence predicted environmental exposure at all if the ranges of the uncertainty in transformation rate constants or attachment efficiencies fall below the critical values at which PECs are no longer sensi-

tive to these physicochemical properties (Fig. 3). The concept of critical transformation rate constants explains the uncertainties in modelled concentrations of poorly and highly soluble metallic ENPs, *i.e.* the dissolution rate of highly soluble ENPs is identified as a significant source of uncertainty in predicted environmental exposure, but this is not the case for poorly soluble ENPs.[13,32,74,75] In addition, the concept of critical attachment efficiencies explains model simulations of stable carbonaceous ENPs that reside in the water column as a free species,[27,30] *i.e.* the attachment efficiencies between natural particles and reduced graphene oxide (2×10^{-7})[27] and multiwalled CNTs (0.79×10^{-6}–1.83×10^{-6})[30] are measured to be below critical ones, so that the free species are simulated to account for more than 95–99% of the total ENP mass.[27,30] As such, the concept of critical attachment efficiencies and transformation rate constants can be used for a necessary simplification of the environmental exposure estimation of nanomaterials.[74]

Implications for risk assessment of nanomaterials

The direct relationships between the physicochemical properties of ENPs and their predicted environmental exposure emphasize the need to include nano-specific fate modelling in environmental exposure and risk assessment (ERA).[32,76,77] Fate modelling is however only part of the information required to fulfil regulatory requirements in the overall approach to ERA,[74] as *e.g.* set under REACH.[78,79] Other aspects include guidance on and standardised methods for deriving the required physicochemical properties and the environmental release categories for estimating the emission to air, soil and water compartments.[80,81] This type of information is needed before a fate model can be applied to estimate the PEC as part of exposure assessment.[80] The indicated critical transformation rate constants and attachment efficiencies (Fig. 3) provide valuable insight in the required accuracy of measurement methods such as for measuring the transformation rate constant and attachment efficiency or dispersion stability.[39,74,82] For ENPs with transformation rate constants above the here identified critical transformation rate constant, a dominant mass fraction (>0.5) of the emitted ENPs will eventually dissolve species once a steady state is reached.[49,69] The need for further testing on ENPs could then be restricted at the screening level stage to focus on the transformation product (*e.g.* dissolved form) instead of the ENP form. Here depending on the time required to reach steady state in an environmental compartment, the critical transformation rate constant ranges between 7.2×10^{-13}–1.7×10^{-6} s^{-1} (Fig. 3). This means for instance that ENPs in water with a transformation rate constant above 1.7×10^{-6} s^{-1} are expected to be primarily in the transformed form. The need for further ecotoxicity testing of the ENP form can be reduced in cases at which both the predicted environmental exposure to the transformed form outweighs the exposure to the ENP form and the predicted no effect threshold of the transformed form is lower than that of the ENP form. Similarly, the critical

attachment efficiencies provide insight in the species of ENP that is expected to be present in the different environmental compartments and thus is relevant to assess with regards to potential effects, the free or hetero-agglomerated ENP species. ENPs with attachment efficiencies below the critical attachment efficiency are expected to be present in the free ENP species. Due to variations in the composition of environmental media, the critical attachment efficiencies range between 8.8×10^{-10}–2.5×10^{-4}. Attachment efficiencies below 7.5×10^{-5} will for instance in water result in ENPs being present primarily as the free, non-agglomerated, species.[27] For ENPs with attachment efficiencies between 7.5×10^{-5} and 1.6×10^{-4} the presence in a free state depends on various other variables, but at attachment efficiencies higher than 1.6×10^{-4} ENPs are again expected to be primarily present as the aggregated or attached species. For the sediment and soil compartment, the critical transformation rate constant and attachment efficiency are much lower because the time to reach steady state in these compartments is longer due to longer residence times. This means that transformations have a longer time to reach equilibrium. In applying such cut-offs with the aim of driving further testing in ERA, this aspect of time needs to be taken into account, *e.g.* by setting a limit to the equilibration time relevant for ERA. Eventually the PEC is compared to a predicted ecotoxicological effect threshold concentration to characterise the risk. This also means that such a threshold concentration should include the relevant ENP species, which in turn means that testing conditions need to be such that the relevant ENP species is taken into account in the effect assessment.[74] When other ENP species are relevant to include in the ERA, other than free and heteroagglomerated ENPs, the analysis should be extended to include those new species and derive the critical reaction rate constants for the new speciation processes, *e.g.* for phototransformation of graphene oxide to reduced graphene oxide.[27]

Nonetheless, the sensitivity analysis performed on SB4N reveals a complex dilemma of which ENP species to prioritize in environmental risk assessment, since (i) ecotoxicity tests are designed for free ENPs but predicted environmental concentrations of free ENPs can be low compared to other species, (ii) ENPs hetero-aggregated with natural colloids can comprise a major fraction in the environment that may be bioavailable, but limited ecotoxicity testing data are available for these ENP species,[77] and (iii) the coarse-attached ENPs are simulated to be most persistent but it is unclear whether they can be treated as inert and least harmful. However, novel insights that generally apply to all ENPs are also gained from the sensitivity analysis are helpful in solving the dilemma: (i) critical attachment efficiencies indicate at which cut-off limit ENPs persist as free pristine particles, (ii) large fractions of bioavailable ENPs are specifically predicted to be present upon emission to the atmosphere and the water column, and (iii) the persistence of ENPs in soil can be expressed as a simple function of transformation rate constant and attachment efficiency.

Conclusions

Setting priorities in environmental risk assessment of ENPs by accounting for the physicochemical properties that yield the highest environmental exposure estimates is not yet straight-forward. A considerable effort in reducing the complexity is already included in screening level multimedia fate models such as SB4N by accounting for ENP speciation patterns, emissions and transport to multiple compartments. Transformation rate constants and attachment efficiencies are the most important properties driving the simulated environmental fate and exposure, but these are also the properties that are most complex to characterize.[47] As such, the model sensitivity analyses performed on SB4N emphasizes the relevance of developing testing guidelines for ENP transformation and attachment behaviour in environmental media.[39,74,82]

Tools for predicting environmental exposure concentrations for risk assessment are readily available, however a full ERA of ENPs remains a complex exercise for now, but environmental fate and speciation modelling deliver insightful results for further development of ERA approaches.

Conflicts of interest

There are no conflicts of interest to declare.

Acknowledgements

References

1 L. C. Abott and A. D. Maynard, Exposure Assessment Approaches for Engineered Nanomaterials, *Risk Anal.*, 2010, **30**, 1634–1644.

2 A. A. Keller, S. McFerran, A. Lazareva and S. Suh, Global life cycle releases of engineered nanomaterials, *J. Nanopart. Res.*, 2013, **15**, 1692–1708.

3 I. Corsi, G. N. Cherr, H. S. Lenihan, J. Labille, M. Hassellov, L. Canesi, F. Dondero, G. Frenzilli, D. Hristozov, V. Puntes, C. D. Torre, A. Pinsino, G. Libralato, A. Marcomini, E. Sabbioni and V. Matranga, Common Strategies and Technologies for the Ecosafety Assessment and Design of Nanomaterials Entering the Marine Environment, *ACS Nano*, 2014, **8**, 9694–9709.

4 A. R. Kohler and C. Som, Environmental and Health Implications of Nanotechnology—Have Innovators Learned the Lessons from Past Experiences?, *Hum. Ecol. Risk Assess.*, 2008, **14**, 512–531.

5 S. J. Klaine, P. J. J. Alvarez, G. E. Batley, T. F. Fernandes, R. D. Handy, D. Y. Lyon, S. Mahendra, M. J. Mclaughlin and

This journal is © The Royal Society of Chemistry 2019

Environ. Sci.: Nano, 2019, **6**, 2049–2060 | **2057**

J. R. Lead, Nanomaterials in the environment: behavior, fate, bioavailability, and effects, *Environ. Toxicol. Chem.*, 2008, **27**, 1825–1851.

6 M. Siegrist, A. Wiek, A. Helland and H. Kastenholz, Risks and nanotechnology: the public is more concerned than experts and industry, *Nat. Nanotechnol.*, 2007, **2**, 67.

7 B. Nowack and T. D. Bucheli, Occurrence, behavior and effects of nanoparticles in the environment, *Environ. Pollut.*, 2007, **150**, 5–22.

8 A. Praetorius, R. Arvidsson, S. Molander and M. Scheringer, Facing complexity through informed simplifications: a research agenda for aquatic exposure assessment of nanoparticles, *Environ. Sci.: Processes Impacts*, 2013, **15**, 161–168.

9 M. Park, E. Bleeker, W. Brand, F. Cassee, M. v. Elk, I. Gosens, W. d. Jong, J. Meesters, W. Peijnenburg, J. Quik, R. Vandebriel and A. Sips, Considerations for safe innovation: The case of graphene, *ACS Nano*, 2017, **11**, 9574–9593.

10 C. Som, M. Berges, Q. Chaudhry, M. Dusinska, T. F. Fernandes, S. I. Olsen and B. Nowack, The importance of life cycle concepts for the development of safe nanoproducts, *Toxicology*, 2010, **269**, 160–169.

11 B. Nowack, J. F. Ranville, S. Diamond, J. A. Gallego-Urrea, C. Metcalfe, J. Rose, N. Horne, A. A. Koelmans and S. J. Klaine, Potential scenarios for nanomaterial release and subsequent alteration in the environment, *Environ. Toxicol. Chem.*, 2012, **31**, 50–59.

12 M. Baalousha, G. Cornelis, T. A. J. Kuhlbusch, I. Lynch, C. Nickel, W. Peijnenburg and N. W. v. d. Brink, Modeling nanomaterial fate and uptake in the environment: current knowledge and future trends, *Environ. Sci.: Nano*, 2016, **3**, 323–345.

13 H. H. Liu and Y. Cohen, Multimedia environmental distribution of engineered nanomaterials, *Environ. Sci. Technol.*, 2014, **48**, 3281–3292.

14 H. H. Liu, M. Bilal, Y. Cohen, A. Lazareva and A. A. Keller, Regional multimedia distribution of nanomaterials and associated exposures: A software platform, *2014 IEEE International Conference on Bioinformatics and Biomedicine*, 2014, pp. 10–17.

15 J. A. Meesters, A. A. Koelmans, J. T. K. Quik, A. J. Hendriks and D. v. d. Meent, Multimedia Modeling of Engineered Nanoparticles with SimpleBox4nano: Model Definition and Evaluation, *Environ. Sci. Technol.*, 2014, **48**, 5726–5736.

16 A. L. Dale, E. A. Casman, G. V. Lowry, J. R. Lead, E. Viparelli and M. Baalousha, Modeling Nanomaterial Environmental Fate in Aquatic Systems, *Environ. Sci. Technol.*, 2015, **49**, 2587–2593.

17 A. L. Dale, G. V. Lowry and E. A. Casman, Modeling Nanosilver Transformations in Freshwater Sediments, *Environ. Sci. Technol.*, 2013, **47**, 12920–12928.

18 R. Arvidsson, S. Molander, B. A. Sanden and M. Hassellov, Challenges in Exposure Modeling of Nanoparticles in Aquatic Environments, *Hum. Ecol. Risk Assess.*, 2011, **17**, 245–262.

19 F. Gottschalk, T. Sun and B. Nowack, Environmental concentrations of engineered nanomaterials: Review of modeling and analytical studies, *Environ. Pollut.*, 2013, **181**, 287–300.

20 F. Gottschalk, T. Sonderer, R. W. Scholz and B. Nowack, Modeled Environmental Concentrations of Engineered Nanomaterials (TiO2, ZnO, Ag, CNT, Fullerenes) for Different Regions, *Environ. Sci. Technol.*, 2009, **43**, 9216–9222.

21 F. Gottschalk, R. W. Scholz and B. Nowack, Probabilistic material flow modeling for assessing the environmental exposure to compounds: Methodology and an application to engineered nano-TiO2 particles, *Environ. Model. Softw.*, 2010, **25**, 320–332.

22 T. Y. Sun, F. Gottschalk, K. Hungerbühler and B. Nowack, Comprehensive probabilistic modelling of environmental emissions of engineered nanomaterials, *Environ. Pollut.*, 2014, **185**, 69–76.

23 N. C. Mueller and B. Nowack, Exposure Modeling of Engineered Nanoparticles in the Environment, *Environ. Sci. Technol.*, 2008, **42**, 4447–4453.

24 J. T. K. Quik, J. J. M. d. Klein and A. A. Koelmans, Spatially explicit fate modelling of nanomaterials in natural waters, *Water Res.*, 2015, **80**, 200–208.

25 H. H. Liu, M. Bilal, A. Lazareva, A. Keller and Y. Cohen, Simulation tool for assessing the release and environmental distribution of nanomaterials, *Beilstein J. Nanotechnol.*, 2015, **6**, 938–951.

26 K. Garner, S. Suh and A. Keller, Assessing the Risk of Engineered Nanomaterials in the Environment: Development and Application of the nanoFate Model, *Environ. Sci. Technol.*, 2017, **51**, 5541–5551.

27 Y. Han, C. D. Knightes, D. Bouchard, R. Zepp, B. Avant, H.-S. Hsieh, X. Chang, B. Acrey, W. M. Henderson and J. Spear, Simulating graphene oxide nanomaterial phototransformation and transport in surface water, *Environ. Sci.: Nano*, 2019, **6**, 180–194.

28 B. Avant, D. Bouchard, X. Chang, H.-S. Hsieh, B. Acrey, Y. Han, J. Spear, R. Zepp and C. D. Knightes, Environmental fate of multiwalled carbon nanotubes and graphene oxide across different aquatic systems, *NanoImpact*, 2019, **13**, 1–12.

29 C. D. Knightes, R. B. Ambrose Jr, B. Avant, Y. Han, B. Acrey, D. Bouchard, R. Zepp and T. Wool, Modeling framework for simulating concentrations of solute chemicals, nanoparticles, and solids in surface waters and sediments: WASP 8 Advanced Toxicant Module, *Environ. Model. Softw.*, 2019, **111**, 444–458.

30 D. Bouchard, C. D. Knightes, X. Chang and B. Avant, Simulating multiwalled carbon nanotube transport in surface water systems using the water quality analysis simulation program (WASP), *Environ. Sci. Technol.*, 2017, **51**, 11174–11184.

31 R. Jacobs, J. A. J. Meesters, C. J. F. ter Braak, D. Van de Meent and H. Van der Voet, Combining exposure and effect modeling into an integrated probabilistic environmental risk assessment for nanoparticles, *Environ. Toxicol. Chem.*, 2016, **35**, 2958–2967.

32 J. A. J. Meesters, A. A. Koelmans, J. T. K. Quik, A. J. Hendriks and D. Van de Meent, Multimedia environmental fate and

speciation of engineered nanoparticles: a probabilistic modeling approach, *Environ. Sci.: Nano*, 2016, **3**, 715–727.

33 B. Nowack, Evaluation of environmental exposure models for engineered nanomaterials in a regulatory context, *NanoImpact*, 2017, **8**, 38–47.

34 D. Hristozov, S. Gottardo, E. Semenzin, A. Oomen, P. Bos, W. Peijnenburg, M. v. Tongeren, B. Nowack, N. Hunt, A. Brunelli, J. J. Scott-Fordsmand, L. Tran and A. Marcomini, Frameworks and tools for risk assessment of manufactured nanomaterials, *Environ. Int.*, 2016, **95**, 36–53.

35 R. J. H. Williams, S. Harrison, V. Keller, J. Kuenen, S. Lofts, A. Praetorius, C. Svendsen, L. C. Vermeulen and J. van Wijnen, Models for assessing engineered nanomaterial fate and behaviour in the aquatic environment, *Curr. Opin. Environ. Sustain.*, 2019, **36**, 105–115.

36 A. A. P. Markus, J. R. Parsons, E. W. M. Roex, P. de Voogt and R. Laane, Modelling the Release, Transport and Fate of Engineered Nanoparticles in the Aquatic Environment - A Review, *Rev. Environ. Contam. Toxicol.*, 2017, **243**, 53–87.

37 A. S. Baun, P. Sayre, K. G. Steinhäuser and J. Rose, Regulatory relevant and reliable methods and data for determining the environmental fate of manufactured nanomaterials, *NanoImpact*, 2017, **8**, 1–10.

38 M. F. Bundschuh, J. Filser, S. Luderwald, M. S. McKee, G. Metreveli, G. E. Schaumann, R. Schulz and S. Wagner, Nanoparticles in the environment: where do we come from, where do we go to?, *Environ. Sci. Eur.*, 2017, **30**, DOI: 10.1186/s12302-018-0132-6.

39 K. Rasmussen, H. Rauscher, A. Mech, J. R. Sintes, D. Gilliland, M. González, P. Kearns, K. Moss, M. Visser, M. Groenewold and E. A. J. Bleeker, Physico-chemical properties of manufactured nanomaterials - Characterisation and relevant methods. An outlook based on the OECD Testing Programme, *Regul. Toxicol. Pharmacol.*, 2017, **92**, 8–28.

40 K. Ettrup, A. Kounina, S. F. Hansen, J. A. J. Meesters, E. B. Vea and A. Laurent, Development of Comparative Toxicity Potentials of TiO2 Nanoparticles for Use in Life Cycle Assessment, *Environ. Sci. Technol.*, 2017, **51**, 4027–4037.

41 J. T. K. Quik, M. C. Stuart, M. Wouterse, W. Peijnenburg, A. J. Hendriks and D. V. D. Meent, Natural colloids are the dominant factor in the sedimentation of nanoparticles, *Environ. Toxicol. Chem.*, 2012, **31**, 1019–1022.

42 I. Velzeboer, J. T. K. Quik, D. Van de Meent and A. A. Koelmans, Rapid settling of nanoparticles due to heteroaggregation with suspended sediment, *Environ. Toxicol. Chem.*, 2014, **33**, 1766–1773.

43 A. Praetorius, M. Scheringer and K. Hungerbühler, Development of Environmental Fate Models for Engineered Nanoparticles A Case Study of TiO2 Nanoparticles in the Rhine River, *Environ. Sci. Technol.*, 2012, **46**, 6705–6713.

44 N. Sani-Kast, M. Scheringer, D. Slomberg, J. Labille, A. Praetorius, P. Ollivier and K. Hungerbühler, Addressing the complexity of water chemistry in environmental fate modeling for engineered nanoparticles, *Sci. Total Environ.*, 2015, **535**, 150–159.

45 A. L. Dale, G. V. Lowry and E. A. Casman, Stream Dynamics and Chemical Transformations Control the Environmental Fate of Silver and Zinc Oxide Nanoparticles in a Watershed-Scale Model, *Environ. Sci. Technol.*, 2015, **49**, 7285–7293.

46 J. T. K. Quik, D. Van de Meent and A. A. Koelmans, Simplifying modeling of nanoparticle aggregation–sedimentation behavior in environmental systems: A theoretical analysis, *Water Res.*, 2014, **62**, 193–201.

47 K. L. Garner and A. A. Keller, Emerging patterns for engineered nanomaterials in the environment: a review of fate and toxicity studies, *J. Nanopart. Res.*, 2014, **16**, 1–28.

48 A. J. Tiwari and L. C. Mar, The Role of Atmospheric Transformations in Determining Environmental Impacts of Carbonaceous Nanoparticles, *J. Environ. Qual.*, 2010, **39**, 1883–1895.

49 D. Mackay and E. Webster, Environmental Persistence of Chemicals, *Environ. Sci. Pollut. Res.*, 2006, **13**, 43–49.

50 M. Bilal, H. Liu, R. Liu and Y. Cohen, Bayesian network as a support tool for rapid query of the environmental multimedia distribution of nanomaterials, *Nanoscale*, 2017, **9**, 4162–4174.

51 A. Praetorius, N. Tufenkji, K. U. Goss, M. Scheringer, F. Von der Kammer and M. Elimelech, The road to nowhere: equilibrium partition coefficients for nanoparticles, *Environ. Sci.: Nano*, 2014, **1**, 317–323.

52 W. J. Peijnenburg, M. Baalousha, J. Chen, Q. Chaudry, F. Von der Kammer, T. A. Kuhlbusch and Z. Wang, A Review of the Properties and Processes Determining the Fate of Engineered Nanomaterials in the Aquatic Environment, *Crit. Rev. Environ. Sci. Technol.*, 2015, **45**, 2084–2134.

53 C. O. Hendren, M. Lowry, K. D. Grieger, E. S. Money, J. M. Johnston, M. R. Wiesner and S. M. Beaulieu, Modeling Approaches for Characterizing and Evaluating Environmental Exposure to Engineered Nanomaterials in Support of Risk-Based Decision Making, *Environ. Sci. Technol.*, 2013, **47**, 1190–1205.

54 C. O. M. Hendren, X. Mesnard, J. Droge and M. R. Wiesner, Estimating production data for five engineered nanomaterials as a basis for exposure assessment, *Environ. Sci. Technol.*, 2011, **45**, 2562–2569.

55 C. Powers, G. Dana, P. Gillespie, M. Gwinn, C. Ogilvie Hendren, T. Long, A. Wang and J. Davis, Comprehensive environmental assessment: a meta-assessment approach, *Environ. Sci. Technol.*, 2012, **46**, 9202–9208.

56 J. A. J. Meesters, A. A. Koelmans, J. T. K. Quik, A. J. Hendriks and D. Van de Meent, Multimedia modeling of engineered nanoparticles with SimpleBox4nano: model definition and evaluation, *Environ. Sci. Technol.*, 2014, **48**, 5726–5736.

57 E. I. D. T. Oracle, *Crystal Ball User's Guide*, Report 11.1.2.3, Oracle America, Inc., Redwood City, 2013.

58 L. J. Brandes, H. d. Hollander and D. v. d. Meent, *Simplebox 2.0: a nested multimedia fate model for evaluating the environmental fate of chemicals*, Report 719101029, 1996.

59 J. T. K. Quik, J. A. Vonk, S. F. Hansen, A. Baun and D. v. d. Meent, How to assess exposure of aquatic organisms to manufactured nanoparticles, *Environ. Int.*, 2011, **37**, 1068–1077.

60 J. R. Lead, W. Davison, J. Hamilton-Taylor and J. Buffle, Characterizing colloidal material in natural waters, *Aquat. Geochem.*, 1997, **3**, 213–232.

61 E. A. J. Bleeker, W. H. d. Jong, R. E. Geertsma, M. Groenewold, E. H. W. Heugens, M. Koers-Jacquemijns, D. v. d. Meent, J. R. Popma, A. G. Rietveld, S. W. P. Wijnhoven, F. R. Cassee and A. G. Oomen, Considerations on the EU definition of a nanomaterial: Science to support policy making, *Regul. Toxicol. Pharmacol.*, 2013, **65**, 119–125.

62 M. E. Pettitt and J. R. Lead, Minimum physicochemical characterisation requirements for nanomaterial regulation, *Environ. Int.*, 2013, **52**, 41–50.

63 A. R. Petosa, D. P. Jaisi, I. R. Quevedo, M. Elimelech and N. Tufenkji, Aggregation and Deposition of Engineered Nanomaterials in Aquatic Environments: Role of Physicochemical Interactions, *Environ. Sci. Technol.*, 2010, **44**, 6532–6549.

64 A. L. Dale, G. V. Lowry and E. A. Casman, Much ado about α: reframing the debate over appropriate fate descriptors in nanoparticle environmental risk modeling, *Environ. Sci.: Nano*, 2015, **2**, 27–32.

65 L. Bergstrom, Hamaker constants of inorganic materials, *Adv. Colloid Interface Sci.*, 1997, **70**, 125–169.

66 ECHA, European Chemical Agency. Guidance on information requirements and chemical safety assessment Appendix R.7.13-2: Environmental risk assessment for metals and metal compounds, *Guidance for the implementation of REACH*, 2008.

67 A. A. Koelmans, N. J. Diepens, I. Velzeboer, E. Besseling, J. T. K. Quik and D. van de Meent, Guidance for the prognostic risk assessment of nanomaterials in aquatic ecosystems, *Sci. Total Environ.*, 2015, **535**, 141–149.

68 R. Jaenicke, *Aerosol cloud-climate interactions*, Academic Press, San Diego, 1993.

69 D. V. d. Meent, A. Hollander, W. Peijnenburg and T. Breure, in *Ecological Impacts of Toxic Chemicals*, ed. F. Sanchez-Bayo and P. J. v. d. Brink, Bentham Science Publishers, Oak Park, 2011, pp. 13–42.

70 ECHA, *Guidance in a Nutshell Chemical Safety Assessment*, 2009.

71 ECHA, *Guidance on information requirements and chemical safety assessment*, 2012.

72 J. T. K. Quik, *PhD thesis*, Radboud University Nijmegen, 2013.

73 G. G. Stokes, *On the effect of internal friction of fluids on the motion of pendulums*, Translation Cambridge Philosophical Society, 1850, vol. IX, p. 8.

74 P. A. Holden, J. L. Gardea-Torresdey, F. Klaessig, R. F. Turco, M. Mortimer, K. Hund-Rinke, E. A. Cohen Hubal, D. Avery, D. Barceló, R. Behra, Y. Cohen, L. Deydier-Stephan, P. L. Ferguson, T. F. Fernandes, B. Herr Harthorn, W. M. Henderson, R. A. Hoke, D. Hristozov, J. M. Johnston, A. B. Kane, L. Kapustka, A. A. Keller, H. S. Lenihan, W. Lovell, C. J. Murphy, R. M. Nisbet, E. J. Petersen, E. R. Salinas, M. Scheringer, M. Sharma, D. E. Speed, Y. Sultan, P. Westerhoff, J. C. White, M. R. Wiesner, E. M. Wong, B. Xing, M. Steele Horan, H. A. Godwin and A. E. Nel, Considerations of Environmentally Relevant Test Conditions for Improved Evaluation of Ecological Hazards of Engineered Nanomaterials, *Environ. Sci. Technol.*, 2016, **50**, 6124–6145.

75 F. Gottschalk, C. Lassen, J. Kjoelholt, F. Christensen and B. Nowack, Modeling Flows and Concentrations of Nine Engineered Nanomaterials in the Danish Environment, *Int. J. Environ. Res. Public Health*, 2015, **12**, 5581–5602.

76 R. Jacobs, J. A. J. Meesters, C. T. F. Braak, D. v. d. Meent and H. v. d. Voet, Combining exposure and effect modeling into an integrated probabilistic environmental risk assessment for nanoparticles, *Environ. Toxicol. Chem.*, 2016, **35**(12), 2958–2967.

77 A. A. Koelmans, N. J. Diepens, I. Velzeboer, E. Besseling, J. T. K. Quik and D. Van de Meent, Guidance for the prognostic risk assessment of nanomaterials in aquatic ecosystems, *Sci. Total Environ.*, 2015, **535**, 141–149.

78 R. Hjorth, L. M. Skjolding, S. N. Sørensen and A. Baun, Regulatory adequacy of aquatic ecotoxicity testing of nanomaterials, *NanoImpact*, 2017, **8**, 28–37.

79 S. F. Hansen, S. N. Sørensen, L. M. Skjolding, N. B. Hartmann and A. Baun, Revising REACH guidance on information requirements and chemical safety assessment for engineered nanomaterials for aquatic ecotoxicity endpoints: recommendations from the EnvNano project, *Environ. Sci. Eur.*, 2017, **29**, DOI: 10.1186/s12302-017-0111-3.

80 ECHA, *Guidance on information requirements and chemical safety assessment, Chapter R.16: Environmental Exposure Estimation, Version 3.0*, European Chemicals Agency (ECHA), Helsinki, Finland, 2016.

81 I. Lynch and B. Hazebrouck, Engineered nanomaterial mechanisms of interactions with living systems and the environment: a universal framework for safe nanotechnology, 2015, http://nanomile.eu-vri.eu/filehandler.ashx?file=13404.

82 K. Rasmussen, M. González, P. Kearns, J. R. Sintes, F. Rossi and P. Sayre, Review of achievements of the OECD Working Party on Manufactured Nanomaterials' Testing and Assessment Programme. From exploratory testing to test guidelines, *Regul. Toxicol. Pharmacol.*, 2016, **74**, 147–160.

2060 | *Environ. Sci.: Nano*, 2019, **6**, 2049–2060

This journal is © The Royal Society of Chemistry 2019